Reducing the computational complexity of WiFi-based passive radar processing

Marco Di Seglio[†], Francesca Filippini[†], Kevin Chetty[††], Fabiola Colone[†]

[†] DIET Department., Sapienza University of Rome, Via Eudossiana, 18 - 00184 Rome, Italy
email: {marco.diseglio, francesca.filippini, fabiola.colone}@uniroma1.it

[††] Department of Security & Crime Science. University College London, Torrington Place, London, UK
email: k.chetty@ucl.ac.uk

Abstract— **WiFi-based passive radar is considered in this paper as an effective technology for short range monitoring applications. Aiming at limiting its complexity and enhancing its suitability for civilian applications, appropriate modifications are proposed to the signal processing scheme originally designed for such sensor. Specifically, we show that a simple inversion in the order of the main processing stages, namely clutter cancellation and range compression, allows to both reduce the number of floating-point operations and relax the requirements on the data management. Moreover, the use of a reciprocal filter in lieu of a matched filter to implement the range compression stage is proved to yield a further simplification in the resulting processing scheme along with additional benefits in terms of achievable performance in the considered application. The alternative processing schemes are compared in terms of computational burden and the effectiveness of the proposed cost-effective solutions is proved against experimental datasets.**

Keywords—WiFi-based passive radar, reciprocal filter, computational load, short range surveillance.

I. INTRODUCTION

Several studies have recently investigated the use of passive radar (PR) in short-range monitoring applications of small private or public areas [1][2]. To this purpose they have looked at the parasitical exploitation of RF emitters able to guarantee the persistent illumination of the areas of interest, though with a limited power density. A quite appropriate choice is offered by transmitters for networking, which may allow for the implementation of a PR for the surveillance of metropolitan and local areas [3]-[6].

With particular reference to local area and indoor applications, the use of modern WLAN transmissions has been investigated and appropriate signal processing strategies have been designed for detecting and localizing moving targets against the competing background, namely the direct signal from the transmitter, its multipath replicas and the receiver noise [7]-[11]. The effectiveness of such approaches has been demonstrated in several experimental tests against drones, vehicles and people. However, given the large bandwidth of the waveforms of opportunity (minimum 20MHz) the conventional signal processing schemes set quite demanding requirements in terms of computational complexity. This limitation has to be carefully addressed in order to enable practical implementation of WiFi-based PR in civilian applications where low-cost, compactness, real-time operation and easy deployment represent the driving factors in the system design.

In this paper, we investigate possible modifications to the conventional signal processing scheme presented in [7]

aimed at reducing the computational load and the complexity of the signal processing architecture.

To this purpose, by taking into account the characteristics of the WiFi transmissions, which are of a pulsed type, we first propose a re-ordering of the most demanding signal processing blocks, i.e., those responsible for (i) the adaptive cancellation of unwanted signal contributions from the transmitter and the stationary scene and (ii) the range-Doppler map evaluation, particularly the range compression stage. The simple inversion in the order used to perform these operations is shown to reduce the computational load and simplify the data management.

Then we resort to a reciprocal filter (RpF) instead of of a conventional matched filter (MF) to implement the range compression stage. Along with the well-known advantage of a remarkable sidelobes control capability for the resulting range-Doppler response [12]-[14], in this paper a RpF-based range compression is shown to provide additional benefits for the specific sensor subject of this study. Specifically, the use of RpF is investigated for WiFi-based PR as a means to simplify the adaptive estimation of the cancellation filter coefficients [15] thus further reducing the computational cost of the resulting signal processing scheme.

The paper is organized as follows. The conventional processing scheme for a WiFi-based PR is recalled in Section II. The revised signal processing architecture is illustrated in Section III, in which the most demanding signal processing blocks are rearranged more effectively. The range compression based on a RpF is introduced in Section IV and its benefits are illustrated in terms of computational complexity. Section V compares the alternative processing schemes in terms of computational load and their effectiveness is tested against experimental data. Finally, we draw our conclusions in Section VI.

II. CONVENTIONAL WiFi-BASED PR PROCESSING SCHEME

A WiFi-based passive radar exploits the pulsed type transmissions of a WiFi access point (AP) as a source of opportunity to detect and localize targets in the monitored area. Let us consider a burst of N_p WiFi packets included within a coherent processing interval (CPI). Assuming that each packet encompasses N_s samples taken at sampling frequency f_s, we denote as $s^{(p)}[n]$, $n = 0, ..., N_s - 1$, the discrete time version of the surveillance signal collected for the p-th packet transmission, $p = 0, ..., N_p - 1$. Along with the surveillance signal, a good copy of the transmitted waveform, namely the reference signal $r^{(p)}[n]$, is needed by

the receiver to guarantee an effective operation of the passive radar. In a semi-cooperative scenario where the operator has access to the WiFi AP, the reference signal can be directly measured . Otherwise, the reference signal must be extracted from the signal collected by the surveillance antenna, specifically by demodulating and re-modulating the received packet $s^{(p)}[n]$, according to the employed IEEE 802.11 Standard.

A conventional signal processing chain [7] is sketched in Fig. 1 for a passive radar exploiting WiFi packets of a single modulation type from the ones adopted in the IEEE 802.11 Standards. As a first stage, the collected signals are fed into a pre-processing block. This stage encompasses the extraction of the WiFi packets from the received data stream and their selection based on the adopted modulation scheme. Then, the extracted packets undergo the clutter cancellation stage [15], aimed at mitigating the stationary scene contribution while preserving slowly moving targets echoes. Among the possible strategies, an effective solution is represented by the Extensive Cancellation Algorithm (ECA) and its modified versions [15]. According to the ECA-based approaches, properly scaled and delayed replicas of the reference signal are subtracted from the surveillance signal, as follows:

$$s_0^{(p)}[n] = s^{(p)}[n] - \sum_{k=0}^{K-1} \hat{\alpha}_k^{(p)} r^{(p)}[n-k] \qquad (1)$$
$$n = 0, \dots, N_s - 1, \; p = 0, \dots, N_p - 1$$

where K is the cancellation filter length, set according to the maximum expected delay for the multipath reflections while the coefficients $\hat{\boldsymbol{\alpha}}^{(p)} = \left[\hat{\alpha}_0^{(p)} \; \hat{\alpha}_1^{(p)} \; \dots \; \hat{\alpha}_{K-1}^{(p)} \right]^T$ are evaluated by resorting to a Least Square (LS) approach that minimizes the power of the signal at the output of the filter $s_0^{(p)}[n]$. In the more general case, the cancellation filter coefficients are updated n_B times along the CPI and are defined as:

$$\hat{\boldsymbol{\alpha}}^{(p)} = \left[\hat{\mathbf{M}}^{(p)} \right]^{-1} \hat{\mathbf{v}}^{(p)} \qquad (2)$$

where $\hat{\mathbf{M}}^{(p)}$ is a $K \times K$ Toeplitz matrix and $\hat{\mathbf{v}}^{(p)}$ is a $K \times 1$ vector whose generic elements are defined as

$$\hat{m}_{lk}^{(p)} = \sum_{p \in I(q)} \sum_{n=0}^{N_s-1} r^{*(p)}[n-l] r^{(p)}[n-k] \qquad (3)$$

$$\hat{v}_l^{(p)} = \sum_{p \in I(q)} \sum_{n=0}^{N_s-1} r^{*(p)}[n-l] s^{(p)}[n] \qquad (4)$$

$$(l, k = 0, \dots, K-1)$$

being $I(q)$ the set of indices corresponding to the signal packets used for the estimation of the filter coefficients to be used at the q-th batch, $q = 0, \dots, n_B - 1$, with $P_B(q) = |I(q)|$. Based on the experimental analyses reported in the literature [7], a reasonable choice is to update the cancellation filter coefficients at each packet, i.e., $n_B = N_p$. The signal packets at the output of (1) then undergo the matched filter (MF) based range compression stage that evaluates the cross-
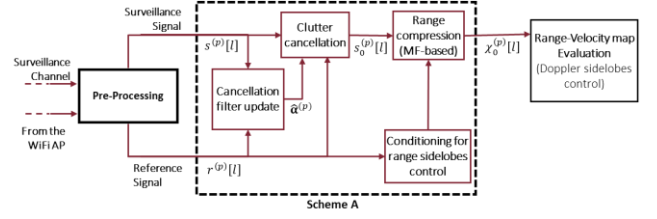

Fig. 1 Signal processing scheme for a WiFi-based passive radar

correlation between the clutter cancelled surveillance signal and the reference signal on a packet-by-packet basis:

$$\chi_0^{(p)}[l] = \sum_{n=0}^{N_s-1} r^{*(p)}[n-l] \, s_0^{(p)}[n] \qquad (5)$$

Finally, the results obtained for all the N_p available packets within the CPI are coherently integrated according to a bank of filters tuned to different target bistatic Doppler values, spaced by Δf, namely different slopes for the target motion induced linear phase law, providing the final bistatic range-velocity map $\psi[l, m]$ to be exploited for target detection and localization.

This processing scheme, referred to in the following as Scheme A, has been extensively tested and shown to be effective for the application at hand [7].

However, it is characterized by a high computational complexity that might prevent its application, especially when real-time operations are required. To illustrate this point we have decomposed the overall cost into three main components:

- Cancellation filter coefficient evaluation: The cost required for the estimation of the coefficients $\hat{\boldsymbol{\alpha}}^{(p)}$ (see eq. (2)), including the estimation of $\hat{\mathbf{M}}^{(p)}$ and $\hat{\mathbf{v}}^{(p)}$ and the inversion of $\hat{\mathbf{M}}^{(p)}$;
- Clutter cancellation: the cost required for the application of the estimated filter coefficients (see eq. (1)).
- Range compression: the cost required for the evaluation of the cross-correlation between the surveillance and the reference signal (see eq. (7)).

The computational burden expected for scheme A is reported in Table I in terms of floating-point operations (FLOPs) needed for each of the three components above, expressed as a function of the relevant parameters. We assume that (i) the cardinality of $I(q)$ is constant along the batches and equal to P_B, (ii) a complex multiplication requires 6 FLOPs and a complex addition requires 2 FLOPs. Note that, when the output of a complex multiplication is expected to be real, the required number of FLOPs decreases to 3. Depending on the employed parameters, some of the considered processing stages might be performed more efficiently in the frequency domain by resorting to an FFT-based implementation rather than in the time domain. Therefore, we report the two alternative implementations in the two columns of Table I. Also, we note that the data rate at the input and output of the clutter cancellation stage is $2N_s f_p$, where f_p is the average packet transmission rate, yielding no reduction of the data rate until the output of the range compression where it is reduced to $N_r f_p$.

TABLE I COMPUTATIONAL COMPLEXITY OF SCHEME A

Processing stage	Scheme A - time implementation	Scheme A - FFT-based implementation
Canc. filter update (along the CPI)	$4KN_p(4N_s - 1)$ $+ 4Kn_B(P_B - 1)$ $+ 2n_B[4K^2 + 4$ $\cdot O(K^3) - K]$	$10N_pN_s \log_2 N_s + 9N_pN_s$ $+ n_B[7.5N_s \log_2 N_s$ $+ 4(P_B - 1)N_s + 8 \cdot O(K^3)$ $+ 48 - 2K]$
Clutter cancellation	$8KN_pN_s$	$5n_BN_s \log_2 N_s + 8N_pN_s$
Range compression	$N_RN_p(8N_s - 2)$	$5N_pN_s \log_2 N_s + 6N_pN_s$

In this work, we aim at modifying the described signal processing scheme with the purpose of lowering the overall computational complexity reported in Table I and simplify its implementation.

III. MODIFIED PROCESSING SCHEME

The computational complexity presented in Section II can be lowered by observing that some of the operations performed for the clutter cancellation and the range compression stages are in common and could be performed just once if the corresponding processing blocks are properly arranged. In other words, using eq. (1) in (5), the output of the cancellation stage can be written as

$$\chi_0^{(p)}[l] = \chi^{(p)}[l] - \sum_{k=0}^{K-1} \alpha_k \chi_r^{(p)}[k - l] \qquad (6)$$

where $\chi^{(p)}[l]$ and $\chi_r^{(p)}[l]$ are the range compressed versions of the input signal and the reference signal, respectively

$$\chi^{(p)}[l] = \sum_{n=0}^{N_s-1} r^{*(p)}[n - l] \, s^{(p)}[n] \qquad (7)$$

$$\chi_r^{(p)}[l] = \sum_{n=0}^{N_s-1} r^{*(p)}[n - l] \, r^{(p)}[n]$$

$$\cong \sum_{n=0}^{N_s-1} r^{*(p)}[n - (l + k)] \, r^{(p)}[n - k] \qquad (8)$$

Therefore, based on (6), the clutter cancelled range compressed signal for the p-th packet is computed as a combination of the corresponding range compressed input signals. In addition, based on (7) and (8), the cancellation filter coefficient in (3) and (4) can be rewritten as

$$m_{k,l}^{(p)} = \sum_{p \in I(q)} \chi_r^{(p)}[k - l] \qquad (9)$$

$$v_l^{(p)} = \sum_{p \in I(q)} \chi^{(p)}[k] \qquad (10)$$

Based on these observations, the range compression stage can be applied once before the clutter cancellation stage on a packet-by-packet basis. The corresponding outputs are then used to evaluate the cancellation filter coefficients, and a clutter cancelled output is obtained by linearly combining the range compressed signals with the filter coefficients $\hat{\alpha}^{(p)}$.
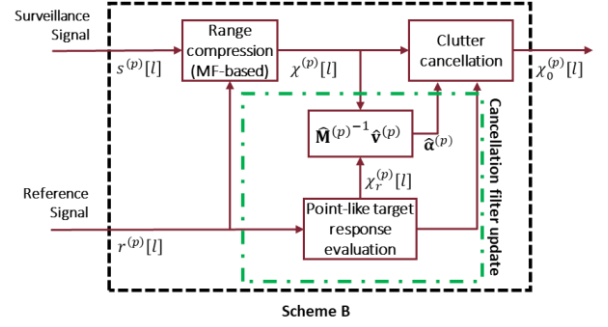

Fig. 2: Modified processing scheme

The new processing chain, referred to in the following as Scheme B, is sketched in Fig. 2 and represents a less costly version of the scheme A.

The computational burden required by the new scheme obtained by simply exchanging the positions of the range compression and disturbance cancellation stages is reported in the first column of Table II. Note that in this case we only report the most convenient implementation of this scheme, which takes advantage of the FFT speed only for the range compression stage. By comparing Table I and Table II, the computational complexity reduction offered by scheme B with respect to scheme A is noticeable in both the cancellation filter coefficients update stage and the clutter cancellation block, now limited to the range bins of interest. Therefore, the decrease will be much more apparent as n_B and N_s grow. For instance, for $K = N_R = 15$, $n_B = N_p = 1000$, and $N_s = 640$, the reduction is of approx. 53%.

Moreover, the possibility of truncating the output of auto- and cross-correlations to a limited number of range bins of interest significantly relaxes data management requirement, lowering the data rate at the output of the range compression stage to $2N_Rf_p$, with a reduction of N_s/N_R compared to the output of the first stage of scheme A. Clearly, the greater is the packet length and the smaller is the number of observed range bins, the higher is the reduction. For instance, assuming that the typical values of N_R are below 30 for the application at hand, the minimum expected decrease is of approx. 95% for $N_s = 640$, which corresponds to typical OFDM acknowledgment (ACK) packets. Then, the data rate at the output of the clutter cancellation stage is further reduced to N_Rf_p.

Despite the reduction offered by this approach, the overall computational load is still high as it is mainly driven by the range compression stage. Therefore, Section IV is devoted to further simplify the processing scheme and devise an alternative and more efficient solution.

TABLE II COMPUTATIONAL COMPLEXITY OF MODIFIED PROCESSING SCHEMES

Processing stage	Scheme B	Scheme C
Canc. filter Update (along the CPI)	$2n_B[4O(K^3) + 4K^2 - K]$ $+ 4Kn_B(P_B - 1)$	$2Kn_B(P_B - 1)$ $+ 2n_B(4K^2 - K)$
Clutter cancellation	$8KN_pN_R$	$8KN_pN_R$
Range compression	$17.5N_pN_s \log_2 N_s$ $+ 9N_pN_s$	$15N_pN_s \log_2 N_s + 6N_pN_s$

IV. RECIPROCAL FILTER BASED RANGE COMPRESSION

Based on the considerations above, we investigate in this Section, the use of the RpF [12]-[14] in lieu of the MF to operate the range compression stage as a mean to further simplify the signal processing architecture.

Let $S^{(p)}[m]$ and $R^{(p)}[m]$ represent the Discrete Fourier Transform (DFT) of the surveillance and reference signals at the p-th packet, respectively, i.e,

$$S^{(p)}[m] = DFT\{s^{(p)}[n]\}$$
$$R^{(p)}[m] = DFT\{r^{(p)}[n]\}$$

$$(11)$$

Based on these definitions, the output of the RpF-based range compression stage and point-like target response provided by the RpF at the p-th packet can be evaluated as

$$\bar{\chi}^{(p)}[l] = IDFT\left\{\frac{S^{(p)}[m]}{R^{(p)}[m]} \cdot rect_{\left|\frac{B}{f_s}N_s\right|}[m]\right\} \quad (12)$$

$$\bar{\chi}_r^{(p)}[l] = IDFT\left\{\frac{R^{(p)}[m]}{R^{(p)}[m]} \cdot rect_{\left|\frac{B}{f_s}N_s\right|}[m]\right\}$$

$$= \frac{\sin\left(\pi\frac{l}{N_s}\left\lfloor\frac{B}{f_s}N_s\right\rfloor\right)}{\sin\left(\pi\frac{l}{N_s}\right)} = \eta[l; B \ ] \quad (13)$$

Note that, in order to to avoid the issues due to overweighting possibly caused by the RpF, we limit its application to the useful bandwidth of the signal of opportunity, i.e., $B = 16.6$ MHz for OFDM modulated packets, forcing the left and right tails of the packet spectrum to be zero. Once the outputs of the RpF-based range compression have been obtained, the conventional ECA-based approaches could be applied for clutter cancellation. However, from eq. (13), we observe that the application of the RpF to the reference signal completely removes the dependency on the transmitted signals. Therefore, an alternative approach for the cancellation filter evaluation is suggested, that leverages the data-independent characteristics of the point-like target response at the p-th packet $\bar{\chi}_r^{(p)}[l]$.

In fact, based on eqs. (12)(13), one can modify eq.(6) as

$$\bar{\chi}_0^{(p)}[l] = \bar{\chi}^{(p)}[l] - \sum_{k=0}^{K-1} \hat{\alpha}_k^{(p)} \eta[l - k; B] \quad (14)$$

where coefficients $\hat{\alpha}^{(p)}$ are evaluated using the clairvoyant version of matrix $\mathbf{M}^{(p)} = \mathbf{M}$ whose generic element is given by

$$m_{lk}^{(p)} = m_{lk} = P_B \, \eta[l - k; B] \quad (15)$$

Therefore, the estimation of the cancellation filter coefficients $\hat{\alpha}^{(p)}$ to be applied at the p-th packet can be simplified as

$$\hat{\alpha}^{(p)} = \mathbf{M}^{-1}\hat{\mathbf{v}}^{(p)} \quad (16)$$

Moreover, being the point-like target response independent on the data and a priori known, there is no longer need for it to be computed.
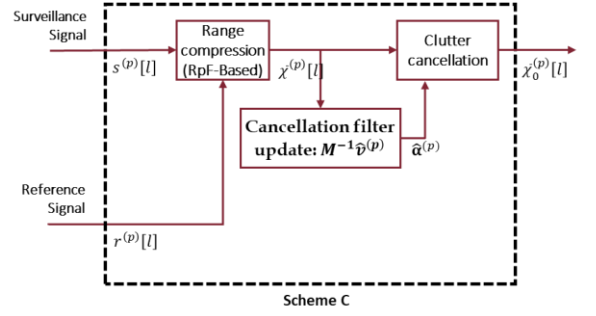

Fig. 3 RpF-based processing scheme

This solution is referred to as ECA-*a priori*, and the overall obtained processing scheme, referred to as Scheme C, is sketched in Fig. 3 while its computational burden is reported in the second column of Table II. As for Scheme B, also in this case we only report the least costly implementation among the time and frequency versions. Note that in this case, the cost of the range compression stage increases due to the need to evaluate the RpF coefficients. However, such additional cost is partly compensated by the fact that there is no need to evaluate the point-like target response of the RpF which is constant across packets and a-priori known. Therefore, in this case, the data rate at the output of the range compression is immediately reduced to $N_R f_p$, which corresponds to a reduction of $2N_s/N_R$ with respect to the first stage of scheme A. As an example, for the same parameters are before, i.e., $N_s = 640$ and $N_R = 30$, the data rate at the output of the first processing stage of scheme C is 97.6% lower than scheme A.

Moreover, note that, with the ECA-*a priori* approach, the evaluation, and the inversion of matrix $\mathbf{M}$ are no longer needed, thus significantly limiting the cost associated to the cancellation stage, and in particular, the cost needed for the cancellation filter update. Finally, the lack of need for matrix inversions enables the implementation of this strategy also on devices where the inversion of a matrix can represent a challenge, such as FPGA.

V. EXTENSIVE ANALYSIS AND EXPERIMENTAL RESULTS

To fully comprehend the advantage of the proposed solutions with respect to the conventional scheme A illustrated in Section II, we evaluate in Table III the cost required by the three alternative solutions for a numerical example.

The employed parameters have been selected among the most typically used. Specifically, we set $N_p = 1000$ packets, which would correspond to a CPI = 0.5 s assuming an average interval of 0.5 ms between consecutive packets transmissions and $K = N_R = 15$ range cells. Moreover, we set $n_B = N_p$, namely we update the filter coefficients at each packet using $P_B = 100$ which would correspond to a cancellation notch of 20 Hz which in turn corresponds to ± 1.25 m/s at 2.4 GHz. The WiFi packet length has been set to $N_s = 640$ samples, which is the typical length of an ACK type packet and corresponds to the OFDM packet preamble plus two additional OFDM symbols. One can assume to limit the packet length to a minimum common value in order to have constant N_s along the CPI.

From Table III, we note that

- For the selected set of parameters, the FFT based implementation of scheme A is less convenient than the time implementation. This is due to the required repetition of the FFT and IFFT operations at each of the n_B batches, which in this case correspond to the overall number of packets in the CPI. The outcome would change if, for instance, n_B was reduced to $N_p/3$.

- Both proposed variations of scheme A allow a reduction of the overall cost with respect of the most efficient implementation of scheme A. More precisely, the computational burden reduction obtained with scheme B and scheme C is of approx. 53 % and 68%, respectively.

- The major reduction offered by scheme C is noted on the cancellation filter coefficient update stage, that is respectively one and two orders of magnitude lower than in scheme A and B. The same reduction is not noted on the overall cost since it remains driven by the range compression stage but has significant advantages. For instance, one could think of applying a bank of parallel clutter cancellation stages with different n_B and P_B, aimed at detecting different targets whose velocities set different requirements.

TABLE III COMPUTATIONAL COST COMPARISON FOR NUMERICAL EXAMPLE

Processing stage	Scheme A Time implementation	Scheme A − FFT based implementation	Scheme B	Scheme C
Canc. Filter Update (along the CPI)	$1.59 \cdot 10^8$	$3.92 \cdot 10^8$	$3.47 \cdot 10^7$	$4.74 \cdot 10^6$
Clutter cancellation	$7.68 \cdot 10^7$	$3.49 \cdot 10^7$	$1.80 \cdot 10^6$	$1.80 \cdot 10^6$
Range compression	$7.68 \cdot 10^7$	$3.37 \cdot 10^7$	$1.10 \cdot 10^8$	$9.33 \cdot 10^7$
Overall cost	$3.13 \cdot 10^8$	$4.61 \cdot 10^8$	$1.47 \cdot 10^8$	$9.99 \cdot 10^7$

Finally, to investigate how the obtained advantage varies when changing the relevant processing parameters, we report in Fig. 4 the number of FLOPs versus the CPI, assuming an average interval of 0.5 ms between consecutive packets. Fig. 4(a) and (b) refer to the case of K = 15 and K = 30, respectively. Solid and dashed lines respectively refer to two different values of n_B, referring to the case where the cancellation filter coefficients are updated at each packet (dashed lines) and the case where the coefficients change every three packets (solid lines), while different colors and markers denote the different employed schemes.
Fig. 4 confirms the considerations made on Table III. Moreover, comparing the solid and dashed lines for the three schemes, it is clear that a very frequent update of the cancellation filter coefficients has a significant impact on the overall cost of scheme A (blue lines), while the increase is reduced for scheme B (red lines) and negligible for scheme C (green lines).
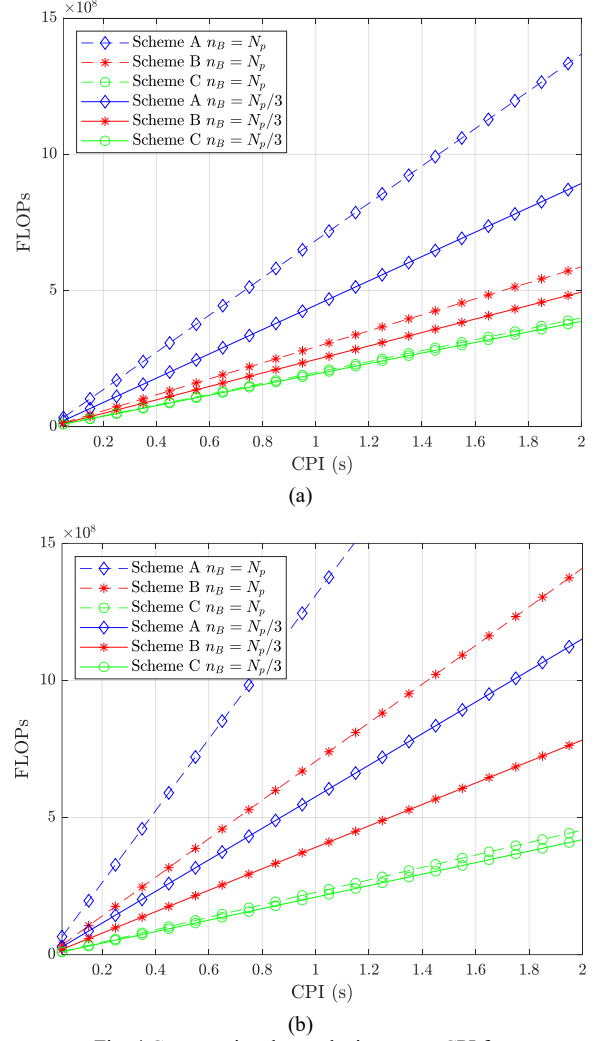

(a)

(b)

Fig. 4 Computational complexity versus CPI for (a) K = 15, (b) K = 30.

This is even more evident when increasing the number of range bins of interests where the multipath reflections are removed, namely comparing Fig. 4(a) and Fig. 4(b). This is expected by observing Table II because the impact of the clutter cancellation filter coefficient evaluation on the overall cost is small for Scheme B and irrelevant for Scheme C, thanks to the ECA-*a priori* approach only enabled by this solution.

To complete this analysis, a dedicated experimental campaign has been carried out in a small outdoor area to test the effectiveness of this scheme, specifically in short-range applications. A commercial wireless AP (TP-Link Archer VR600 AC1600) was used as illuminator of opportunity and connected to a transmitting directive antenna. The AP was configured to transmit packets according to the 802.11n only standard in channel 13 of the WiFi band ($f_0 = 2.472$GHz). One TP-Link TL-ANT2409A antenna was employed to acquire the surveillance signal from the monitored area where two people were present and acted as cooperative human targets walking along radial trajectories in opposite directions, while the transmitted signal was directly collected from the AP.

In Fig. 5 we show the results for one scan obtained with a CPI of 0.5 seconds, during which 1065 OFDM packets are collected.
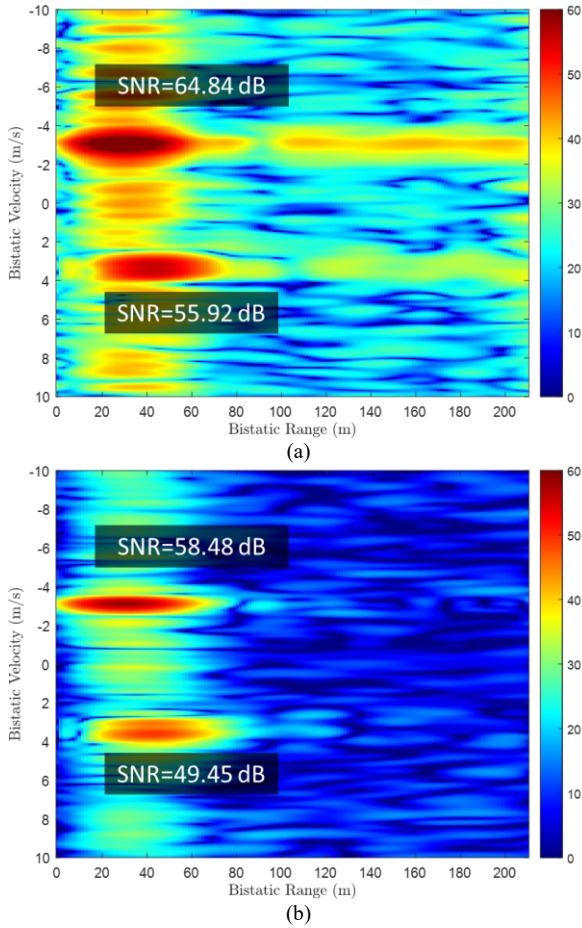
Fig. 5: Bistatic Range-Velocty map for a single CPI using
(a) scheme A and B (b) scheme C

VI. CONCLUSION

In this paper, we propose appropriate modifications to the conventional processing scheme for WiFi based passive radar with the purpose of limiting its overall computational burden and relaxing its data management requirements. A first simplification is obtained with an inversion in the order of the main processing stages, namely clutter cancellation and range compression. Then, we demonstrate that the use of a reciprocal filter for range compression enables further simplifications in the resulting processing scheme while preserving the obtained performance. The alternative processing schemes are compared in terms of computational complexity and the effectiveness of the proposed cost-effective solutions is proved against experimental data.

REFERENCES

[1] F. Colone, "Short-range passive radar potentialities", in "Novel Radar Techniques and Applications Vol. 1: Real Aperture Array Radar, Imaging Radar, and Passive and Multistatic Radar", Ch. 15, pp. 661-718.

[2] P. Samczynski, et al., "Passive Radar as a Part of Critical Infrastructure Protection System," 2018 International Conference on Radar, Brisbane.

[3] A. A. Salah et al., "Feasibility study of LTE signal as a new illuminators of opportunity for passive radar applications," 2013 IEEE International RF and Microwave Conference, 2013, pp. 258-262.

[4] A. Evers and J. A. Jackson, "Analysis of an LTE waveform for radar applications," 2014 IEEE Radar Conference, 2014, pp. 0200-0205.

[5] R. S. Thoma et al., "Cooperative Passive Coherent Location: A Promising 5G Service to Support Road Safety," in IEEE Communications Magazine, vol. 57, no. 9, pp. 86-92, September 2019.

[6] P. Falcone, F. Colone, P. Lombardo, "Potentialities and challenges of WiFi-based passive radar", IEEE Aerosp. Electron. Syst. Mag., vol. 27, no. 11, pp. 15-26, Nov. 2012.

[7] F. Colone, P. Falcone, C. Bongioanni, P. Lombardo, "WiFi-Based Passive Bistatic Radar: Data Processing Schemes and Experimental Results". IEEE Transactions on Aerospace and Electronic Systems. 2012; vol. 48(2), pp. 1061-1079.

[8] D. Pastina, F. Colone, T. Martelli and P. Falcone, "Parasitic Exploitation of Wi-Fi Signals for Indoor Radar Surveillance," in IEEE Transactions on Vehicular Technology, vol. 64, no. 4, pp. 1401-1415, April 2015.

[9] K. Chetty, G. E. Smith and K. Woodbridge, "Through-the-Wall Sensing of Personnel Using Passive Bistatic WiFi Radar at Standoff Distances," in IEEE Transactions on Geoscience and Remote Sensing, vol. 50, no. 4, pp. 1218-1226, April 2012.

[10] S. Rzewuski, K. Kulpa, P. Samczyński, "Duty factor impact on WIFIRAD radar image quality", 2015 IEEE Radar Conference, 2015, pp. 400-405.

[11] H. Sun, L. G. Chia and S. G. Razul, "Through-Wall Human Sensing with WiFi Passive Radar," in IEEE Transactions on Aerospace and Electronic Systems.

[12] M. Glende, "PCL-signal-processing for sidelobe reduction in case of periodical illuminator signals", Proc. Int. Radar Symp., pp. 1-4, 2006.

[13] J. Palmer, H. Harms, S. Searle and L. Davis, "DVB-T passive radar signal processing", IEEE Trans. Signal Process., vol. 61, no. 8, pp. 2116-2126, Apr. 15, 2013.

[14] G. Gassier et al., "A unifying approach for disturbance cancellation and target detection in passive radar using OFDM", IEEE Trans. Signal Process., vol. 64, no. 22, pp. 5959-5971, Nov. 2016.

[15] F. Colone, C. Palmarini, T. Martelli, E. Tilli, "Sliding extensive cancellation algorithm for disturbance removal in passive radar", in IEEE Transactions on Aerospace and Electronic Systems, vol. 52, no. 3, pp. 1309-1326, June 2016.

[16] F. Colone, F.Filippini, M. Di Seglio, K. Chetty, " On the Use of Reciprocal Filter against WiFi packets for passive radar", submitted to IEEE Transactions on Aerospace and Electronic Systems.

Specifically, these figures report the Bistatic Range-Velocity maps scaled for the output noise level to be around 0 dB. Fig. 5(a) is obtained with either scheme A or B which we recall yield identical outputs though with different implementations, while Fig. 5(b) reports the map obtained with scheme C which encompasses a RpF strategy for range compression. The clutter cancellation stage exploits an ECA-S in Fig. 5(a) and its *a priori* version in Fig. 5(b), in both cases with a time interval of 0.05 seconds ($P_B = 115$) for the estimation of the cancellation filter coefficients and an update rate corresponding to the packet rate ($n_B = N_p$). In both subfigures, the targets can be clearly distinguished from the background. In particular, it is worth observing that the ECA-*a priori* preserves a remarkable capability to remove the clutter returns despite the significant reduction in terms of complexity. In addition, we note that scheme C benefits from the nice characteristic of the RpF addressed in technical literature, such as a better sidelobes control in comparison with the MF-based range compression (scheme A and B), offering a much clearer range-Doppler map. It is worth noticing that the RpF-based scheme yields an SNR loss with respect to Scheme A and B, however for the typical power levels of this application, this does not result in a degraded detection performance. Still, this aspect is carefully investigated in [16].